

AN INVESTIGATION ON USING THE FALLING MASS TECHNIQUE FOR DYNAMIC FORCE CALIBRATIONS

Shaker A. Gelany, Gouda M. Mahmoud

National Institute of Standards (NIS), Tersa St, El-Haram, PO Box 136, Code 12211, Giza, Egypt
(✉ shaker9595@yahoo.com, +20 1010 304 830, goudamohamed15@yahoo.com)

Abstract

In this paper, we present an experimental setup developed for the calibration of dynamic force transducers which is based on the drop mass method. The traceability to SI units is realized through well-known mass characteristics and a reference shock accelerometer attached to that mass. Two approaches are proposed to analyse dynamic force employing a drop mass system. One approach depends on the inertial force of a falling mass while the other deals with the work-energy principle. Results of both approaches are then compared to the response of a statically calibrated force transducer. It is shown that the obtained maximum relative deviations between the response of force transducer and the first approach results are 1% while those of the second approach are 2%.

Keywords: calibration, dynamic calibration, impact force, falling weight.

© 2021 Polish Academy of Sciences. All rights reserved

1. Introduction

Dynamic force measurements have spread rapidly in several industrial fields such as process monitoring, material testing and motion control [1–3]. Dynamic force transducers are typically calibrated with static methods and under static conditions due to the lack of standard methods for evaluating the dynamic characteristics of force transducers. Although methods for dynamic calibration of force transducers are not yet well established, there have been several attempts to establish methods for dynamic calibration for force transducers. In dynamic calibration, there must be a method for generating or realizing a dynamic force and also some method for determining the dynamic force realized. The force generator may generate a periodic force (use of electrodynamic shakers) or a transient force (use of impact apparatus) [4–9]. Recently, the falling mass has become one of substantial transient methods for the calibration of dynamic force transducers in which the inertial force of the mass is used as a reference force [10, 11]. This study aims to present an experimental setup of a falling mass system for achieving traceability in dynamic force calibration. The reference force is achieved through well-known mass characteristics and

a standard shock accelerometer attached to that mass. Two approaches are proposed to analyse dynamic force employing a drop mass system. The first approach depends on the inertial force of a falling mass while the second one deals with the work-energy principle.

2. Fundamental of the falling mass technique

The *National Institute of Standards (NIS)* of Egypt has established a *Falling Mass System (FMS)* for dynamic force calibration. The reference force generated by the FMS is determined by two approaches which are described in the following sections:

2.1. First approach

This approach deals with the inertial force. The inertial force acting on the falling mass is determined according to Newton's 2nd law [12]:

$$F(t) = ma(t), \quad (1)$$

where m is the falling mass value and a is the acceleration acting on the falling mass. The layout of the FMS and the basic model of the force transducer is depicted in Fig. 1a.

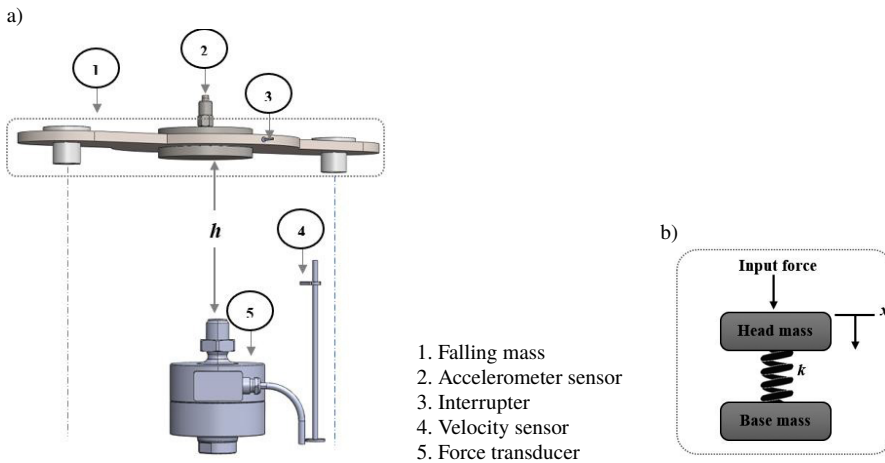


Fig. 1. a) Layout of the falling mass force calibration system; b) Basic model of the force transducer.

2.2. Second approach

This approach is based on the work-energy principle [12]. Starting with (1), we can obtain the relationship between the work done acting on the falling mass and the corresponding change in its kinetic energy. Applying the scalar product of each side of (1) with the velocity v of the falling mass, (2) can be obtained;

$$F \cdot v = ma \cdot v, \quad (2)$$

where $F \cdot v$ is the instantaneous rate at which the force acting on the falling mass is performing work on that mass, taking this into account, (3) is obtained;

$$F \cdot v = \frac{dW}{dt}, \quad (3)$$

where W is the work done on the mass m by the net force acting on it. The right side of (2) $ma \cdot v$, can be written as;

$$ma \cdot v = m \frac{dv}{dt} \cdot v = m \frac{d}{dt} \left(\frac{v \cdot v}{2} \right) = m \frac{d}{dt} \left(\frac{v^2}{2} \right) = \frac{d}{dt} \left(\frac{1}{2}mv^2 \right) = \frac{dK}{dt}, \quad (4)$$

where K is the kinetic energy.

Substituting (3) and (4) into (2), (5) can be obtained:

$$\frac{dW}{dt} = \frac{dK}{dt}, \quad (5)$$

By integrating both sides of (5) with time, (6) can be obtained:

$$W = K_i - K_o, \quad (6)$$

where W is the work done on the falling mass during a time interval beginning at the time t_o and ending at the time t_i . Because the falling mass starts from rest, its kinetic energy K_o is equal to zero. The work done is obtained from the following equation:

$$W = \frac{1}{2}mv_i^2, \quad (7)$$

where m is the falling mass value and v_i is the impact velocity at that moment before impact. The force transducer can be modelled as a mass-spring system as shown in Figure 1b. The force transducer's output signal is considered proportional to the compression of the spring element [11]. While the spring element is compressed from its equilibrium position $x_i = 0$, it can do work as it returns to the initial position. The elastic potential energy could be defined as the work done by the spring element in returning to its reference position and can be obtained from the following equation:

$$W = \int_{x_i}^{x_{\max}} F dx = \frac{1}{2}k(x_i^2 - x_{\max}^2), \quad (8)$$

where F is the elastic force, $F = -kx$, of the spring element, k is the stiffness constant, x_i and x_{\max} are the displacements of the uncompressed and compressed spring. Therefore, W becomes

$$W = \frac{1}{2}Fx. \quad (9)$$

From (7) and (9), (10) can be obtained:

$$\frac{1}{2}mv_i^2 = \frac{1}{2}Fx, \quad (10)$$

where x is the integral of velocity which, in turn, is the integral of acceleration [13].

For measured acceleration $a(t)$, the velocity can be written as:

$$v(t) = v_i - \int_{t_i}^{t_{\max}} a(t) dt, \quad (11)$$

where v_i denotes the falling mass velocity. The displacement which is the integral value of $v(t)$ is expressed as:

$$x(t) = \int_{t_i}^{t_{\max}} v(t) dt . \quad (12)$$

The integration begins at the time $t_i = 0$, the moment of the first contact between the falling mass and force transducer and ends at time $t_{\max} = t$, the moment of falling mass rebounds. The force can be obtained from the following (13):

$$F(t) = \frac{mv_i^2}{x(t)} . \quad (13)$$

3. Experimental setup of the FMS

Figure 2 shows the block diagram and the falling mass system calibration setup. The complete FMS setup consists of a loading frame, a velocity sensor, a force transducer, an accelerometer sensor, and a measurement facility. The loading frame is used to lift the falling mass to a pre-defined height required for generating a certain force. The falling mass is a compound body consisting of a cylindrical mass (2.170 kg), a mass plate (2.007 kg), two bearings (0.100 kg) and an accelerometer sensor (0.005 kg). The total value of the falling mass is equal to 4.280 kg. Two electromagnets are used for attaching the falling mass to the mass lifter. The mass lifter is attached to a ball screw which is controlled by a stepper motor. After releasing the falling mass, it falls along the guiding rods and hits the force transducer.

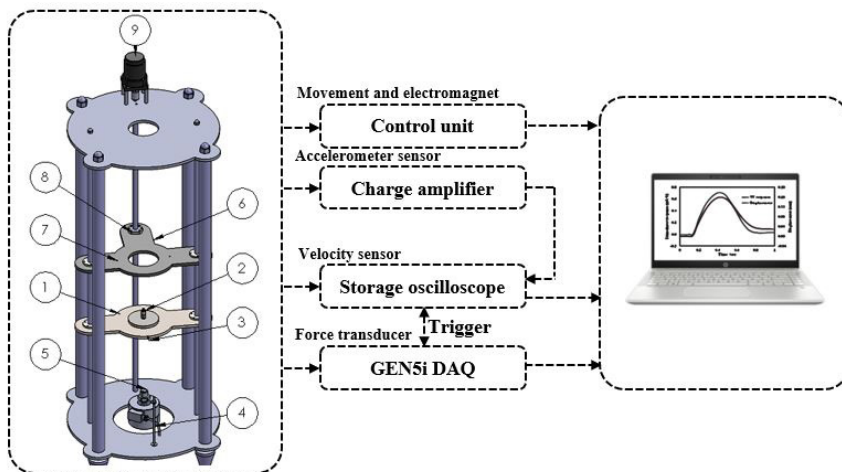


Fig. 2. Block diagram and calibration setup of the FMS: 1 – falling mass, 2 – accelerometer sensor, 3 – interrupter, 4 – velocity sensor, 5 – force transducer, 6 – mass lifter, 7 – electromagnet, 8 – ball screw, 9 – stepper motor.

Figure 3a shows the impacting mass velocity measuring sensor. The impact velocity was measured using a photo interrupter sensor (Vishay type TCST2103) interrupted by an interrupter attached to the falling mass. The impact mass velocity was measured with the photo interrupter sensor in a position very close to the impact on the force transducer.

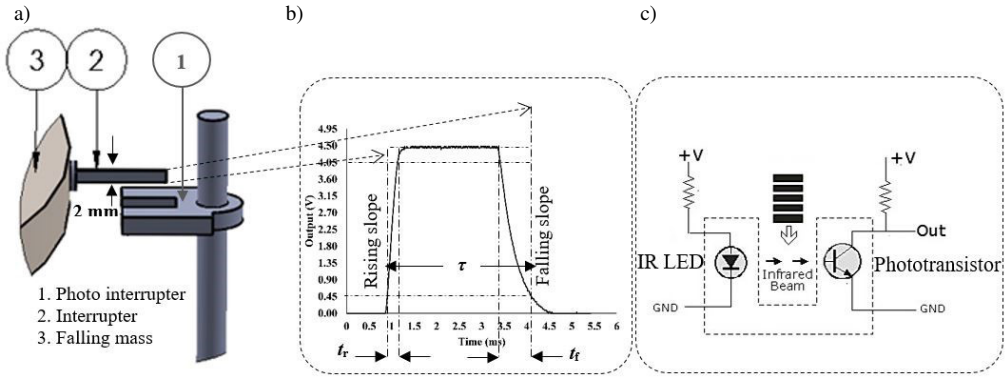


Fig. 3. a) Impact velocity measurement system; b) output signal; c) schematic of the photo interrupter.

The velocity was calculated as $v_i = d/\tau$, where d is the interrupter width and τ is the pulse width between the rising slope to the falling slope.

Figure 3b shows the output signal of the photo interrupter. The pulse signal has asymmetric slopes with a rise time t_r and a fall time t_f of 5% and 15% of the pulse width, respectively. Additionally, the velocity sensor is composed of an infrared emitter (IR LED) and an infrared detector (phototransistor) facing each other, as shown in Fig. 3c. By emitting a beam of IR light, the sensor can detect when an object passes between the emitter and detector, breaking the light beam. The impact velocity sensor's output was connected to an oscilloscope. The estimated uncertainty of the impacting mass velocity is 10%.

Figure 4 shows the mechanical structure and the measurement facility. A high precision force transducer (type U2B, manufactured by HBM) with a nominal force of 50 kN was used in this study. The force transducer was calibrated statically according to ISO 376:2011 and classified as Class 00. The output of the force transducer was connected to a data acquisition system (type GEN5i by HBM). Its maximum sampling rate is 100 MS/s. The acceleration was measured



Fig. 4. Mechanical structure and measurement facility: 1 – mechanical structure, 2 – falling mass, 3 – velocity sensor, 4 – force transducer, 5 – charge amplifier, 6 – oscilloscope, 7 – data acquisition system, 8 – computer.

using a standard shock accelerometer (manufactured by PCB Piezotronics, type 350C03) with a sensitivity of $0.05 \text{ mV}/(\text{m}/\text{s}^2)$. It was fixed tightly on the top surface of the falling mass. The accelerometer sensor's output was connected to a charge amplifier (PCB Piezotronics type 482C54) having a scale factor of $200 \text{ mV}/(\text{m}/\text{s}^2)$. The charge amplifier's output is sampled using a digital storage oscilloscope (model TDS2024B, manufactured by Tektronix) which has a maximum sampling rate of $2 \text{ GS}/\text{s}$.

3.1. Measurement sequence

The FMS is fully automated using a developed LabVIEW program. The measurement sequence starts by setting the machine zero position, where the distance between the lower surface of the impacting mass and the force transducer head is equal to zero. Then the falling mass is lifted to a target height required for generating a certain force. Next, the lifted mass is released by controlling the electromagnets. Subsequently, the oscilloscope and GEN5i start signal sampling once the velocity sensor detects that the interrupter passes between its emitter and detector. Finally, signal processing is executed offline for the recorded signals on the Origin package platform.

4. Results and discussions

The force transducer response was recorded using the GEN5i at a sampling frequency of $100 \text{ kS}/\text{s}$. The test series of 3 measurements for 4 chosen falling heights have been performed with the experimental FMS described in Fig. 2. Figure 5 below shows typical force-time curves given by the FMS for different selected heights. The force pulses are characterized by a pulse width of less than 1 ms and a maximum force from 18 kN to 50 kN .

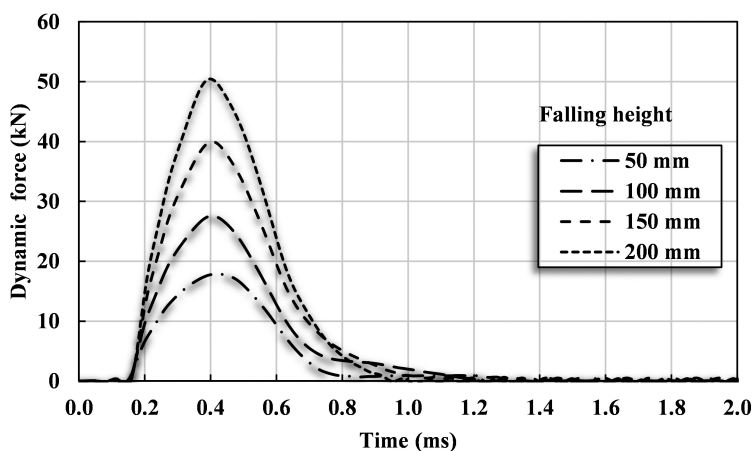


Fig. 5. Force transducer response with time.

Figure 6 shows the accelerometer's original and filtered signal. The acceleration time signal was illustrated for a falling height of 100 mm . When the falling mass strikes the force transducer, an elastic wave is created directly and is transmitted into the force transducer. This wave is also reflected in the falling mass. As the falling mass and the force transducer remain attached during the collision process, the wave's to-and-fro motion leads to oscillations observed in the

accelerometer signal in Fig. 6. The acceleration signal was measured at the sampling rate of 100 kS/s. A *Fast Fourier Transform* (FFT) low pass filter has been applied to the acceleration signal to attenuate the observed oscillations and noise. The acceleration signal is low-pass filtered at a cut-off frequency of 5 kHz.

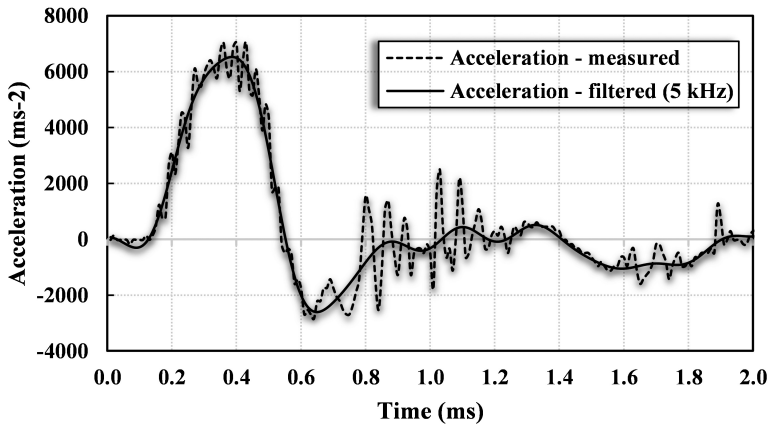


Fig. 6. Accelerometer original and filtered signal.

Table 1 lists the falling mass values and the average maximum acceleration acting on the mass during the collision for different falling heights. Moreover, average maximum values of transducer response and average maximum values of a reference force calculated using (1) are listed. The first approach evaluated using the relative error as a comparison criterion whose results are compared to the response of the force transducer. The obtained relative deviation in (%) is gathered in the last column. The reference force always gives maximum force values slightly bigger than the force transducer. A good agreement was observed between the reference force values and the force transducer values. The relative deviation between the maximum forces remains below 1%.

Table 1. Maximum transducer response and reference force using (1).

Falling height h (mm)	Mass m (kg)	Average maximum acceleration $a(t)$ (m/s^2)	Average maximum reference force F (kN)	Average maximum transducer response (kN)	Relative deviation (%)
50	4.282	4194.160	17.960	17.849	0.6
100	4.282	6457.145	27.651	27.552	0.4
150	4.282	9354.466	40.058	39.920	0.3
200	4.282	11804.418	50.549	50.448	0.2

Similarly, the results of the second approach are compared the response of the force transducer for the same measurements. The second approach uses (13) to calculate the reference force. Table 2 lists the corresponding average measured maximum values of velocity, displacement and reference force. The obtained relative deviation between the maximum forces is exceeds 2% for higher force values.

Table 2. Maximum transducer response and reference force using (13).

Falling height h (mm)	Mass m (kg)	Average velocity v_i (m/s)	Average maximum displacement x_{max} (mm)	Average maximum reference force F (kN)	Average maximum transducer response (kN)	Relative deviation (%)
50	4.282	0.816	0.160	17.820	17.849	0.2
100	4.282	1.205	0.224	27.757	27.552	0.7
150	4.282	1.538	0.251	40.354	39.920	1.1
200	4.282	1.835	0.279	51.679	50.448	2.4

5. Conclusions

An experimental setup of the falling mass technique for the dynamic calibration of force transducers has been presented. Two different approaches for the analysis of the measurement data were successfully tested. The results of both approaches are then compared to the response of a statically calibrated force transducer. It is shown that both calibration methods achieve comparable results.

Acknowledgement

This work has been supported by the National Institute of Standards (NIS), Egypt, through the use of its lab facilities. The support is highly appreciated.

References

- [1] Fujii, Y., Isobe, D., Saito, S., Fujimoto, H., & Miki, Y. (2000). A method for determining the impact force in crash testing. *Mechanical Systems and Signal Processing*, 14(6), 959–965. <https://doi.org/10.1006/mssp.1999.1272>
- [2] Fujii, Y. (2003). A method for calibrating force transducers against oscillation force. *Measurement Science and Technology*, 14(8), 1259–1264. <https://doi.org/10.1088/0957-0233/14/8/310>
- [3] Hjelmgren, J. (2002). *Dynamic Measurement of Force – A Literature Survey* (SP Report 2002:34). SP Swedish National Testing and Research Institute SP Measurement Technology.
- [4] Jun, Y., Yiqing, C., Xuan, H., & Xiao, Y. (2017). Impulse force calibration with dropped weight and laser vibrometer. *IMEKO 23rd TC3, 13th TC5 and 4th TC22 International Conference*, Finland, 19. <https://www.imeko.org/publications/tc3-2017/IMEKO-TC3-2017-030.pdf>
- [5] Kobusch, M., Link, A., Buss, A., & Bruns, T. (2007). Comparison of shock and sine force calibration methods. *IMEKO 20th TC3, 3rd TC16 and 1st TC22 International Conference*, Mexico. <https://www.imeko.org/publications/tc3-2007/IMEKO-TC3-2007-007u.pdf>
- [6] Satria, E., Takita, A., Nasbey, H., Prayogi, I. A., Hendro, H., Djamal, M., & Fujii, Y. (2018). New technique for dynamic calibration of a force transducer using a drop ball tester. *Measurement Science and Technology*, 29(12). <https://doi.org/10.1088/1361-6501/aaeb71>
- [7] Schlegel, C., Kieckenap, G., Glöckner, B., Buß, A., & Kümme, R. (2012). Traceable periodic force calibration. *Metrologia*, 49(3), 224–235. <https://doi.org/10.1088/0026-1394/49/3/224>

- [8] Sivaselvan, M. V., Reinhorn, A. M., Shao, X., & Weinreber, S. (2008). Dynamic force control with hydraulic actuators using added compliance and displacement compensation. *Earthquake Engineering and Structural Dynamics*, 37(15), 1785–1800. <https://doi.org/10.1002/eqe.837>
- [9] Stanford, A. L., & Tanner, J. M. (1985). Work, Power, and Energy. In *Physics for Students of Science and Engineering* (pp. 109–144). Elsevier Inc. <https://doi.org/10.1016/b978-0-12-663380-1.50008-2>
- [10] Vljajic, N., & Chijioko, A. (2017). Traceable calibration and demonstration of a portable dynamic force transfer standard. *Metrologia*, 54(4), S83–S98. <https://doi.org/10.1088/1681-7575/aa75da>
- [11] Yang, Y., Zhao, Y., & Kang, D. (2016). Integration on acceleration signals by adjusting with envelopes. *Journal of Measurements in Engineering*, 4(2), 117–121. <https://www.jvejournals.com/article/16965/pdf>
- [12] Zhang, L., & Kumme, R. (2003). Investigation of interferometric methods for dynamic force measurement. In *XVII IMEKO World Congress, Metrology in the 3rd Millennium*, Croatia, 315–318.
- [13] Zhang, L., Wang, Y., & Zhang, L. (2010). Investigation of calibrating force transducer using sinusoidal force. *AIP Conference Proceedings*, 1253, 395–401. <https://doi.org/10.1063/1.3455481>



Shaker A. Gelany received the Ph.D. degree in Mechanical Design and Production Engineering, Faculty of Engineering, Cairo University, in 2019. He is currently a researcher in Mass, Density and Pressure Metrology Laboratory, National Institute of Standards (NIS), Egypt.



Gouda M. Mahmoud received the Ph.D. degree in Mechanical Design and Production Engineering, Faculty of Engineering, Cairo University, in 2014. He is currently Associate professor of Force & Material Metrology and the Quality Manager of National Institute of Standards (NIS), Egypt.